



HAL
open science

Radio Access Mechanism for Massive Internet of Things Services Over White Spaces

Monica Espinosa, Manuel Perez, Tatiana Zona, Xavier Lagrange

► **To cite this version:**

Monica Espinosa, Manuel Perez, Tatiana Zona, Xavier Lagrange. Radio Access Mechanism for Massive Internet of Things Services Over White Spaces. *IEEE Access*, 2021, 9, pp.120911 - 120923. 10.1109/access.2021.3105131 . hal-03338604

HAL Id: hal-03338604

<https://hal.science/hal-03338604>

Submitted on 9 Sep 2021

HAL is a multi-disciplinary open access archive for the deposit and dissemination of scientific research documents, whether they are published or not. The documents may come from teaching and research institutions in France or abroad, or from public or private research centers.

L'archive ouverte pluridisciplinaire **HAL**, est destinée au dépôt et à la diffusion de documents scientifiques de niveau recherche, publiés ou non, émanant des établissements d'enseignement et de recherche français ou étrangers, des laboratoires publics ou privés.



Distributed under a Creative Commons Attribution 4.0 International License

Received June 25, 2021, accepted July 27, 2021, date of publication August 16, 2021, date of current version September 8, 2021.

Digital Object Identifier 10.1109/ACCESS.2021.3105131

Radio Access Mechanism for Massive Internet of Things Services Over White Spaces

MONICA ESPINOSA¹, (Member, IEEE), MANUEL PÉREZ², (Member, IEEE),
TATIANA ZONA¹, AND XAVIER LAGRANGE³, (Senior Member, IEEE)

¹Department of Telecommunication Engineering, Universidad Santo Tomas, Bogotá 110231, Colombia

²Department of Electronic Engineering, Universidad Javeriana, Bogotá 110231, Colombia

³IMT Atlantique, IRISA UMR CNRS 6074, 35700 Rennes, France

Corresponding author: Monica Espinosa (monica.espinosa@usantotomas.edu.co)

This work was supported in part by the Colombian Ministry of Information and Communications, the Colombian Ministry of Science, Technology and Innovation through the Centro de Excelencia y Apropiación en Internet de las Cosas (CEA-IoT) Project, in part by the Ministry of Science, Technology and Innovation (Ministerio de Ciencia, Tecnología e Innovación Min Ciencias) through the Fondo Nacional de Financiamiento para la Ciencia, la Tecnología y la Innovación Francisco José de Caldas Program under Project FP44842-502-2015, in part by the Ponticia Universidad Javeriana, in part by the Universidad Santo Tomas, and in part by the IMT Atlantique.

ABSTRACT This paper proposes a novel radio access mechanism for massive Internet of Things (IoT) services over TV White Spaces (TVWS). The proposal considers TVWS as the suitable frequency bands for facing the limited-spectrum problem in massive IoT services. The radio access mechanism is based on regulatory policies by interacting with a TVWS Geolocation Database through the Protocol to Access White-Space (PAWS) and using several Master Devices (MD)s. With this approach, IoT devices require neither geolocation receiver in the deployments, nor different frequency bands for initialization process within PAWS. Regarding the evaluation of the radio access mechanism, we explore different types of deployments and coverage areas. This paper also describes the optimization process to obtain the maximum service area, while maintaining an outage probability below a given objective. Moreover, we evaluate the performance of a loaded network with the maximum service area, with respect to a reference case with one MD. We evidence that the average packet loss probability is reduced by 26% when the load is equal to 80% in our proposal.

INDEX TERMS IoT, white spaces, macro-diversity, access.

I. INTRODUCTION

In the last 20 years, the Internet has changed the way people communicate, work and do business. Currently, the Industrial Revolution 4.0 is showing a significant impact on different sectors of the society, such as, energy, transport, health, and manufacture of goods or services [1]–[5]. According to the World Economic Forum (WEF), this revolution has the potential to improve the quality of life of the entire population and one of the best and fastest tools for achieving this is by means of the Internet of Things (IoT) [6]. The IoT paradigm defines things as objects such as household appliances, wearable and means of transport, among others. The concept of IoT was initially defined by the International Telecommunication Union (ITU) in 2005 in the world summit on information society [7]. According to the ITU [8], IoT is defined as a global infrastructure for the information society that enables advanced services by interconnecting physical and virtual

things through the interoperability of the Information and Communication Technologies (ICT).

IoT services are divided into two categories, critical and massive, depending on their criticality and the number of sensors per application [9]. Critical services have high levels of reliability and low latency constraints. In contrast, massive services require low cost terminals and low energy consumption, but are latency tolerant. In terms of network deployment, massive services have substantial challenges regarding scalability and the size of the headers of their communication protocols. In general, IoT devices have wireless access networks that establish a centralized and distributed communication for data transmission to the Internet. Regarding the radioelectric spectrum for IoT, there are challenges such as limited spectrum, scalability and limited bandwidth [10]–[12].

The European Commission concluded that the demand for the IoT radio spectrum has grown exponentially and IoT services need frequency bands below 1 GHz [13]. In our proposal, we consider Television White Spaces (TVWS) as suitable frequency bands below 1 GHz to overcome the

The associate editor coordinating the review of this manuscript and approving it for publication was Xiaolong Li¹.

TABLE 1. Available list of channels.

| Geographic Point | Latitude | Longitude | Available Channels |
|------------------|----------|-----------|--------------------|
| Amazonas | -4,22293 | -69,9837 | 31,32,40-50 |
| Caqueta | 2,56869 | -72,641 | 28-36,38-50 |

limited spectrum problem. According to the spectrum regulation, TVWS are frequencies that have not been allocated in a geographic area. They should be managed with a Geolocation Database (GLDB) that gives the list of available channels into different geographic points. The GLDB is in charge of avoiding interference with the Television (TV) primary users. In countries as Colombia, TVWS are from 470MHz to 698MHz in Ultra High Frequency (UHF) band with channels from 14 to 51. For example, Table 1 shows the list of available channels in two geographic points between Amazonas and Caqueta, two contiguous mostly rural regions in the south of Colombia with an extension of almost 190000 km². Therefore, the available channels are suitable for deployments of massive IoT devices as opportunistic secondary users.

In this paper, first we propose a novel radio access mechanism for IoT massive services, with Dynamic Spectrum Access (DSA) in TV bands, that takes into account the regulatory policies. On the one hand, the radio access mechanism is based on the standard Protocol to Access White-Space (PAWS) and requires no geolocation receiver in the IoT devices when they are located within the deployment area. On the other hand, we propose an architecture with several fixed stations, namely Master Device (MD), which can decode the messages sent by the IoT devices and also provide a beacon channel. Moreover, IoT devices can check their location with this beacon channel.

In the following, we highlight the main contributions of the present research:

- A novel radio access mechanism that allows the deployment of IoT massive services on TVWS frequencies. This radio access mechanism is based on the Protocol to Access White-Space (PAWS), standardized by the Internet Engineering Task Force (IETF), and it requires no geolocation receiver in the IoT devices.
- An analytical model to compute the packet loss probability on the service areas and deployments.
- A performance comparison of several possible deployments and service areas with outage probability equal to 1%.
- Guidelines for service areas of TVWS with respect to the MDs deployment.
- An analytical model to evaluate the performance of a load network considering macro-diversity gain, service areas, and a comparison of the topology with one MD and our proposal with three MDs.

This paper is organized as follows. In Section II, we discuss the relevant literature and background definitions about low power, low cost, low overhead, and scalable wide area networks, in particular about IoT over TVWS through GLDB. In Section III, we describe the model of the outage probability, deployments, reference areas, IoT devices positioning

and packet loss characterization. In Section IV, we evaluate the radio access mechanism with different deployments, service areas, IoT devices positioning and packet loss models. In Section V, we present the results analysis and the deployment rules. In section VI, we outline the main conclusion of the paper.

II. REVIEW AND BACKGROUND DEFINITIONS

The radio access mechanism provides TVWS access for massive IoT services. These IoT services have applications based on sensors and actuators [9]. Besides, IoT services have network requirements such as low cost for massive deployments, low energy consumption, low overhead, extended coverage and scalability. In the review, we consider the aforementioned requirements in radio architectures over TVWS.

A. IoT NETWORK DEPLOYMENTS OVER TV WHITE SPACES

TVWS networks are based on DSA techniques. These techniques find access to available frequencies over licensed bands, such as TV bands. The aim of this access is to avoid interferences with users in licensed bands, namely, primary users. In the case of TV bands, there are policies defined for establishing DSA over these bands of frequencies. These policies are developed taking into account body spectrum regulators through GLDB for coexisting with TV primary users. Moreover, the TVWS users, namely, opportunistic secondary users, must have the available list of frequency channels to access TV bands. In our research, we are focused on how the massive IoT services obtain the available list of frequencies for coexisting with the primary user.

Few works in the literature have addressed the deployment of IoT networks over TVWS. The work in [14] proposes an architecture called Sensor Network Over White Spaces (SNOW). This architecture, which is single hop, is based on Distributed Orthogonal Frequency Division Multiplexing (D-OFDM) and the Carrier-Sense Multiple Access (CSMA) mechanism, where the D-OFDM is used for managing the TVWS bandwidth and CSMA as coexistence method between opportunistic secondary users. The SNOW architecture is focused on coexistence between opportunistic secondary users. Therefore, the authors do not consider this mechanism to obtain the available list of frequencies for massive IoT services. Although the architecture topology in [14] is described in detail, the authors assume that the network base station knows all the end device locations either through manual configuration, which only applies for static sensor nodes, or through some existing Wireless Sensor Network (WSN) localization based on ultrasonic techniques, which does not necessarily guarantee low energy consumption for IoT devices. In this vein, the SNOW topology architecture is a centralized topology, then, for obtaining the available list of frequencies, it has disadvantages in scalability, long payloads and IoT location. Furthermore, the architecture proposal does not consider the use of Quality of Service (QoS) variables for defining the network service and deployments areas. In [15], a framework with dynamic spectrum management

for Machine to Machine (M2M) in Long Term Evolution Advanced (LTE-A) is defined. In this work, a system is proposed considering the radio spectrum policy and spectrum sensing techniques for M2M over LTE-A. The spectrum sensing system is applied to IoT devices and this process does not guarantee low cost and low energy consumption in massive IoT services. Therefore, this study does not consider IoT constraints such as low cost, low energy consumption and scalability. Moreover, the architecture topology is centralized and scalability is not guaranteed in the primary user coexistence.

According to [16], a standard for M2M communication, named Weightless, was born in response to a wide-area machine communications network that meets all the sector requirements. Weightless is designed to enable IoT communications in TVWS. The architecture has a centralized topology and it does not need to define a special mechanism for obtaining the available list of frequencies in massive IoT cases. Finally, it does not consider the QoS with respect to the service areas and deployments supported by PAWS.

Our proposal has features such as long coverage, low energy consumption and small payload, which can be easily related to a Low-Power Wide-Area Network (LPWAN) for IoT deployments. However, in the previous literature review, a complete quantitative comparison of the existing LPWAN technologies with our proposal is not possible, since the main proposal is a radio access framework for massive IoT deployments over TVWS, which can be in general adapted to several network technologies. To better explain our approach, not a quantitative but qualitative comparison was made with the main LPWAN technologies, as shown in Table 2.

The design of a radio access mechanism for massive services over TVWS, for coexisting with primary users and obtaining the available list of frequencies, has challenges related to IoT requirements such as low cost, high energy efficiency, large coverage, small payloads and reasonable good QoS. In the literature, to the best of our knowledge, there is neither a network radio access mechanism proposal that considers DSA in TV bands for massive IoT services, based on PAWS and compliant with regulatory policies, nor a definition of service and deployments areas according to QoS network metrics.

Regarding our radio access mechanism, we reviewed the recommendation made by Internet Engineering Task Force (IETF) to achieve the aim of our functionalities [17]. Besides, the regulatory policies were based on TVWS access through GLDB, which are reviewed and defined in the following sections.

B. TVWS GEOLOCATION DATABASE

Since all TVWS devices have to avoid interference with primary TV users, it is important that these devices follow the radioelectric spectrum regulatory policies. According to these policies, TVWS networks must have a minimum of three components namely GLDB, MD and Slave Device (SD). A set of rules for spectrum access are in the GLDB, which also provides the available list of channels taking into account

the device location, the allocated frequency for TV primary users and the current coexistence conditions. An MD requests the available list of channels to the GLDB and at the same time, interacts with the GLDB on behalf of the SD.

The calculation model in the GLDB is designed according to the management of interference with parameters such as co-channel, adjacent channel, prohibited channels, Height Above the Average Terrain (HAAT), Effective Isotropic Radiated Power (EIRP), antenna height, transmission power, unwanted emissions and frequency bands, among others. Thus, when an available list of channels request arrives at the GLDB, it calculates the conditions for avoiding interference with TV primary users for a requested geographic position. When the GLDB system returns the available list of channels for SD and MD, if the link between the SD and MD has channels in common, both devices can establish communication over TVWS.

The Federal Communications Commission (FCC), in the FCC 04-113, FCC 08-260, FCC 10-174 and FCC 14-144, defined unlicensed operation in the TV Broadcast Bands [18]. The TV stations operate on 6 MHz channels designated from channels 2 to 51 in four bands of frequencies in the Very High Frequency (VHF) and UHF regions of radioelectric spectrum (54-72 MHz, 76-88 MHz, 174-216 MHz and 470-698 MHz). The fixed devices may operate on any available channel within that range, while personal/portable devices may operate only on channels 21 to 51, excluding channel 37 in the following frequencies 512-608 MHz (TV channels 21 to 36) and 614-698 MHz (TV channels 38 to 51) [18]. The fixed White Space Device (WSD) can utilize an external antenna up to 30 meters above the ground and it is allowed to transmit with a higher power up to 4W of EIRP, with a 6 dBi antenna gain. These devices cannot be located at a site where the ground HAAT exceeds 250 meters [19]. Personal/Portable Devices are limited to a maximum EIRP of 100mW or 40mW if the device is operating on an adjacent channel of an occupied TV channel [19].

According to [20], Ofcom defined TVWS in bands of frequencies from 470 to 550 MHz and from 614 to 790 MHz. Besides, Ofcom verified the commercial implementation of the WSD by involving the regulatory bodies, industry stakeholders, and users to verify the process. Ofcom has the technical objective of the correct functioning of WSD, the operation of the GLDB, calculations and operation of the database, the programming of special events in Digital Terrestrial Television (DTT), interference management, and coexistence [21].

Regarding the European regulation in [22], the report number 159 by the Electronic Communications Committee (ECC), within European Conference of Postal and Telecommunications Administrations (CEPT), assumes the GLDB operation in the 470-790 MHz frequency band. In the report, three cognitive techniques are proposed: sensing, GLDB and beacon. In addition, the report number 236 defines the main functions of the framework for TV WSD into the GLDB and TVWS applications [23].

TABLE 2. Comparative analysis with other IoT networks.

| Networks | Type of frequency | Type of coverage | Frequency Band | Comments |
|----------------|---------------------------------------|---------------------------------|---------------------------------------|---|
| SigFox Lora | Unlicensed | Continuous coverage nation-wide | Sub-GHz 865-868 MHz 902-924 MHz | Low cost but overcrowded frequencies |
| NB-IoT | Licensed | Continuous coverage nation-wide | 700-900MHz | High cost to use the frequencies |
| Our Proposal | Dynamic Spectrum Access over TV Bands | Local system | Sub-GHz 470-698 MHz | Need for the list of available channels from a GLDB |

In the Colombian case [24], devices can only use the 470-698 MHz frequency band for two types of communications: point to point and broadcast. Similarly in the communication system, the SD has to use the same transmission channel of the device associated with MD. Before the devices have their own available list of channels, the network uses its own channel (e.g. Industrial, Scientific and Medical (ISM) bands). The MD cannot start neither continue its operation when the list of available channels delivered by the GLDB is empty, thus delivering an error signal to cease the operation. Moreover, the SD will not be able to start neither continue its operation when there is no communication with the MD or when its list of available channels has no common entries with the MD.

C. PAWS

A secondary device should be able to check if a given frequency from a primary user can be used. IETF defined PAWS [17] as a protocol to allow any kind of device to exchange information with a GLDB in order to accomplish the spectrum policy. The network entities in this protocol are master and slave devices where the MD has direct access with GLDB and it sends a request on behalf of the SD. PAWS has different functionalities, namely, initialization, device registration, available spectrum query, device validation and spectrum use. Figure 1 shows the PAWS sequence. In addition, there are messages such as INIT, REGISTRATION and AVAIL SPECTRUM that cannot use TVWS frequencies because the MD and SD do not have an available list of channels yet. For this reason, the network has to use another band of frequencies such as ISM bands. Moreover, the PAWS geolocation information may be a single point or a region described by a polygon [17]. When the MD or SD received the available list of channels, the devices can use the channels taking into account a timestamp defined by PAWS. For instance, in Request for Comments (RFC) 7545 [17], the timestamp is 24 hours. When the timestamp is over, the devices have to renew their available list of channels.

The disadvantages of PAWS for massive IoT services are: (i) messages can be long, (ii) the devices have to report their locations and need bands of frequencies as ISM for their first access to GLDB before knowing the available list of channels, and (iii) there is a scalability issue, because each SD must request independently its available list of channels.

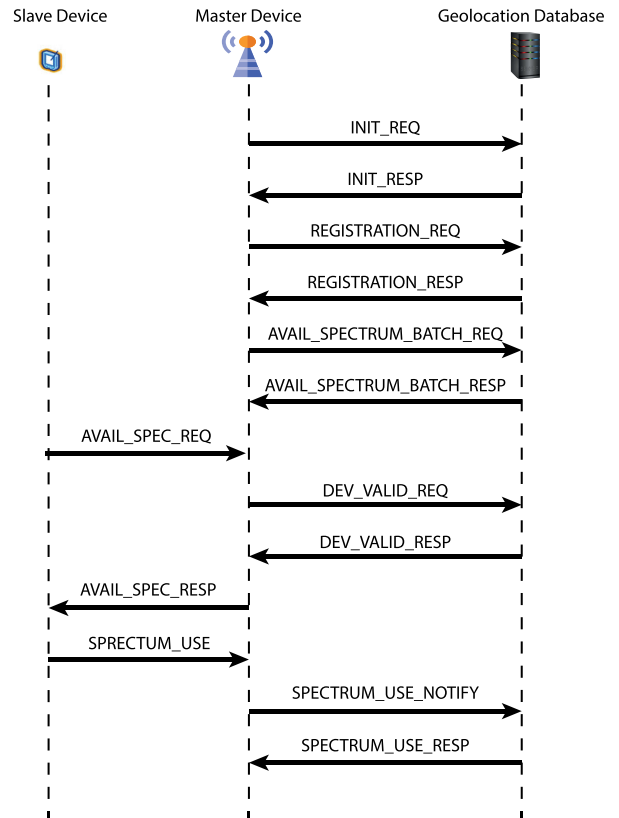


FIGURE 1. PAWS sequence.

D. IoT DEVICES POSITIONING

In our proposal, we applied Observed Time Difference of Arrival (OTDOA) for IoT devices positioning. In this method, the SD (i.e IoT device) measure the Time of Arrival (TOA) signal received from multiple MDs. OTDOA is based on the intersection between hyperbolas, considering difference of time. The intersection between hyperbolas is the desired SD location [25]. In this process, the TOA is calculated for each MD as $t_1 = \tau_2 - \tau_1$, $t_2 = \tau_3 - \tau_1$, and $t_3 = \tau_3 - \tau_2$. Let τ_1 , τ_2 , and τ_3 be the TOA for each MD, respectively.

Regarding IoT implementations, OTDOA is used by laboratories as Ericson [26]. The authors presented simulation with OTDOA, and concluded that the technique is suitable for IoT, due to network scalability. The simulation results in the outdoor IoT case show that the error in position is less than 100 meters in the 70 th percentile.

In [27], the authors made a hardware implementation and a laboratory test-bed for IoT positioning with OTDOA. In the

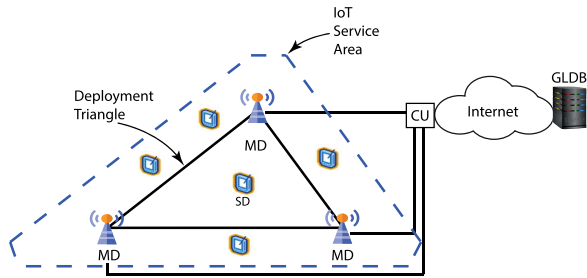


FIGURE 2. Radio architecture.

indoor case, the authors obtained an error equal to 65.5 m with -116 dBm Rx Power.

III. RADIO ACCESS MECHANISM

We propose a radio architecture as depicted in Figure 2. The architecture considers only GLDB to access TVWS. Moreover, in our network, there are four main components: GLDB, Central Unit (CU), MD and SD. The GLDB is the spectrum database and it is compliant with PAWS protocol. The CU is in charge of removing duplicated packets between the MDs and GLDB. Besides, the CU can access GLDB on behalf of each MD. The MD is a tower-mounted transceiver equipped with a geolocation and synchronization receiver. There are at least 3 MDs in a geographical area. The SD includes a simple transceiver that is able to work in the TVWS spectrum but does not need to manage the ISM bands. Although our proposal can work with more than 3 MDs, we only consider in the following the 3-MDs case for the sake of simplicity. Note that the 3-MDs configuration is also the one that minimizes the deployment cost. We call the triangle formed by the three MDs the *deployment triangle*.

A *service area* is defined as a polygon-based area in which a SD can transmit data packets with a given maximum packet loss probability. As shown in Figure 2, the service area is generally a larger polygon than the deployment area. In our proposal, an SD is able to check whether it is in the service area and which frequency can be used. Finally, we propose a radio access mechanism taking into account the radio architecture based on macro-diversity gain and consistent with the PAWS protocol.

The steps for accessing TVWS are shown in Figure 3. The MDs obtain the list of available channels from the GLDB by specifying the service area (i.e. the location of all points that define the polygon). The MDs choose a common channel in this list. Then, they can start the transmission when they are sure that the channel is available.

Each MD transmits a beacon message in a synchronized round robin fashion, as shown in Figure 4. By using OTDOA, a SD can deduce its position without any dedicated geolocation receiver with a certain precision when it is inside the so called *deployment triangle*. OTDOA system degrades its precision when the SD is located outside, so a different geolocation system should be used.

The proposed sequence of messages is shown in Figure 3, which illustrates only one MD out of three. In this new

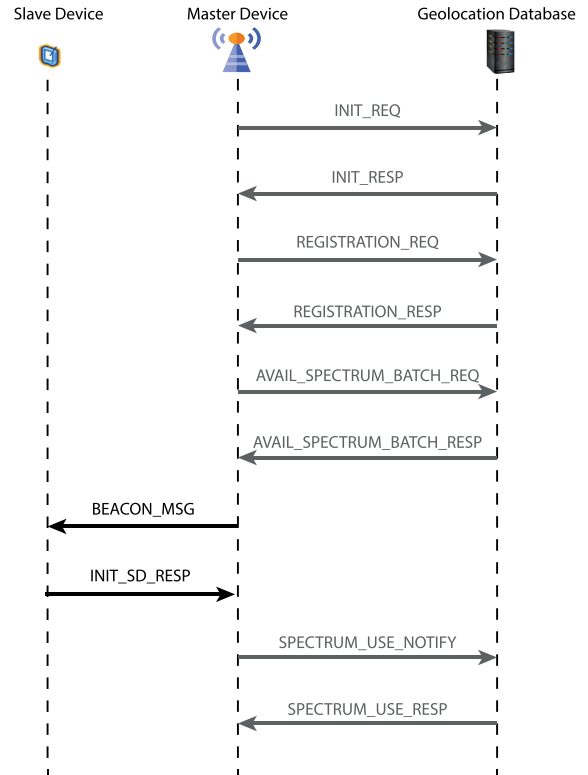


FIGURE 3. Sequences of the radio access mechanism for one master device.

sequence, two messages between the SD and MDs are created, namely BEACON-MSG and INIT-SD-RESP. The BEACON-MSG includes the available list of channels inside the service area, the MD locations and timestamp for accessing TVWS. The INIT-SD-RESP has the SD location and available channels that the SD has selected. Figure 5 illustrates these steps. When the IoT devices are outside to *deployment* and inside the *service area*, they have to use the Global Navigation Satellite System. In this case, the SD can receive the messages for obtaining the available list of channels and then it sends INIT-SD-RESP.

The proposal has the next features: (i) the network is fixed, (ii) the three MDs work on the same frequency, and (iii) a packet transmitted by a SD can be received by any of the three MDs.

IV. EVALUATION OF THE RADIO ACCESS MECHANISM

Intuitively, deploying the MDs in an equilateral triangle maximizes the service area for a given target outage probability. However, operational constraints can make this operation difficult. Therefore, first we consider any type of *deployment triangles*, compute the outage probability in the general case and then deduce *deployment guidelines*. Second, average packet reception models are explored. Moreover, we define the reference case considering shadowing and shadowing with fast fading, and establish a fair comparison with our *deployments* and *service areas*. Third, we define the *deployment rules* taking into account triangle inner angles. Next, we optimize the *services areas* and obtain the corresponding

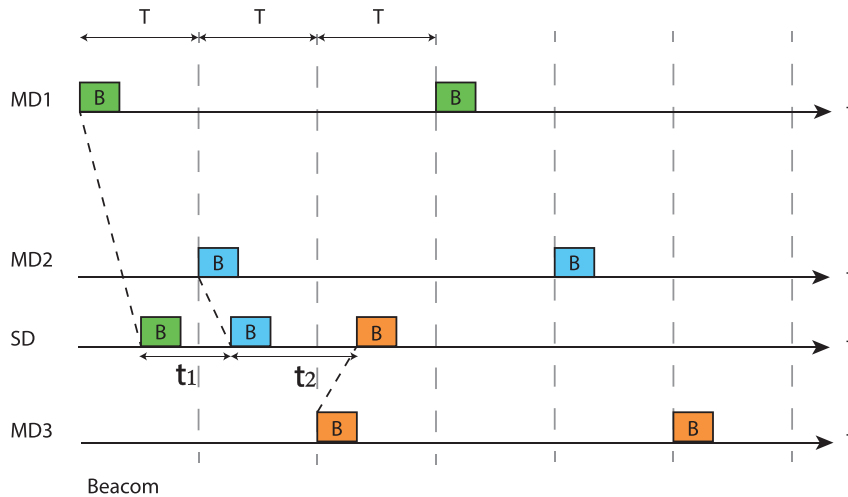


FIGURE 4. Beacon messages.

service areas rules. Then, we evaluate the IoT positioning inside our deployments. Finally, an analysis of a loaded system is presented considering macro-diversity gain.

A. EXPLORING DIFFERENT MASTER DEVICE DEPLOYMENTS

We consider different deployments for the triangle formed by the three MDs. Let (O, N, Q) be the triangle vertices and α, β and δ be the angles of the triangle. Let D be the distance between O and Q as shown in Figure 6.

Without loss of generality, we assume that the relation between each angle is as follows:

$$0 < \delta \leq \beta \leq \alpha. \tag{1}$$

After a few elementary computation steps, it is easy to show that:

$$\begin{aligned} \text{if } \alpha \in \left[\frac{\pi}{3}, \frac{\pi}{2} \right) & \left\{ \begin{aligned} \beta &\in \left[\frac{\pi - \alpha}{2}, \alpha \right] \\ \delta &\in \left[\pi - 2\alpha, \frac{\pi - \alpha}{2} \right] \end{aligned} \right. \\ \text{if } \alpha \in \left[\frac{\pi}{2}, \pi \right) & \left\{ \begin{aligned} \beta &\in \left(\frac{\pi - \alpha}{2}, \pi - \alpha \right] \\ \delta &\in \left(0, \frac{\pi - \alpha}{2} \right] \end{aligned} \right. \end{aligned} \tag{2}$$

There is of course an infinite number of triangles. In order to have a set of representative cases, we only consider angles that are multiples of $\pi/12$, thus $\alpha = \frac{\pi}{3} + \frac{k\pi}{12}$ with $k \in [0, 7]$. Considering possible values of β and δ given by (2), we identified eleven different triangles that are listed in table 3.

The size of the deployment triangle is fixed by choosing D . The area A_d is given by:

$$A_d = \frac{1}{2} D^2 \sin(\delta) \left[\cos(\delta) + \frac{\sin(\delta)}{\tan(\beta)} \right], \tag{3}$$

In this section, we propose an approach for determining the area of the deployments taking into account the distance D and the triangle angles. Figure 6 shows this approach.

B. PROPAGATION MODEL

The propagation channel follows the Okumara-Hata propagation model. Let P_r and P_t be the received and transmitted power, respectively.

$$P_r = P_t \left(\frac{d_0}{d} \right)^\gamma 10^{\frac{\sigma \xi}{10}} \chi \tag{4}$$

where d_0 is a reference distance related to the environment, γ is the propagation exponent, ξ is a standard normal random variable ($\xi = N(0, 1)$), σ is the shadow standard deviation in dB, and χ is an exponential random variable. Note that the shadowing effect is taken into account by ξ and fading by χ .

Fast fading is due to multipath propagation and only occurs in narrow-band systems. When the signal spectrum is larger than the coherence bandwidth, the multi-path effect is addressed by equalization and factor χ can be removed from (4). We consider both cases (i.e. shadowing with fast fading, and shadowing only) because our architecture has no restrictive assumption in the type of transmission technique.

C. PACKET LOSS PROBABILITY ON ONE LINK

The Signal to Interference Plus Noise Ratio (SINR) is given by:

$$\theta = \frac{P_r}{N + I}, \tag{5}$$

where N is the background noise power and I is the interference generated by all users that are simultaneously transmitting. The background noise is $N = f_{NF} kTW$ where f_{NF} is the noise factor, k the Boltzmann constant, T is the temperature in Kelvin and W the bandwidth.

For the outage probability computation, we assume low load conditions. Hence, there is no interference and only background noise. The SINR is given by:

$$\theta = \frac{P_r}{N}, \tag{6}$$

Since we consider a simple reception model a packet is correctly decoded if the Signal to Noise Ratio (SNR) is

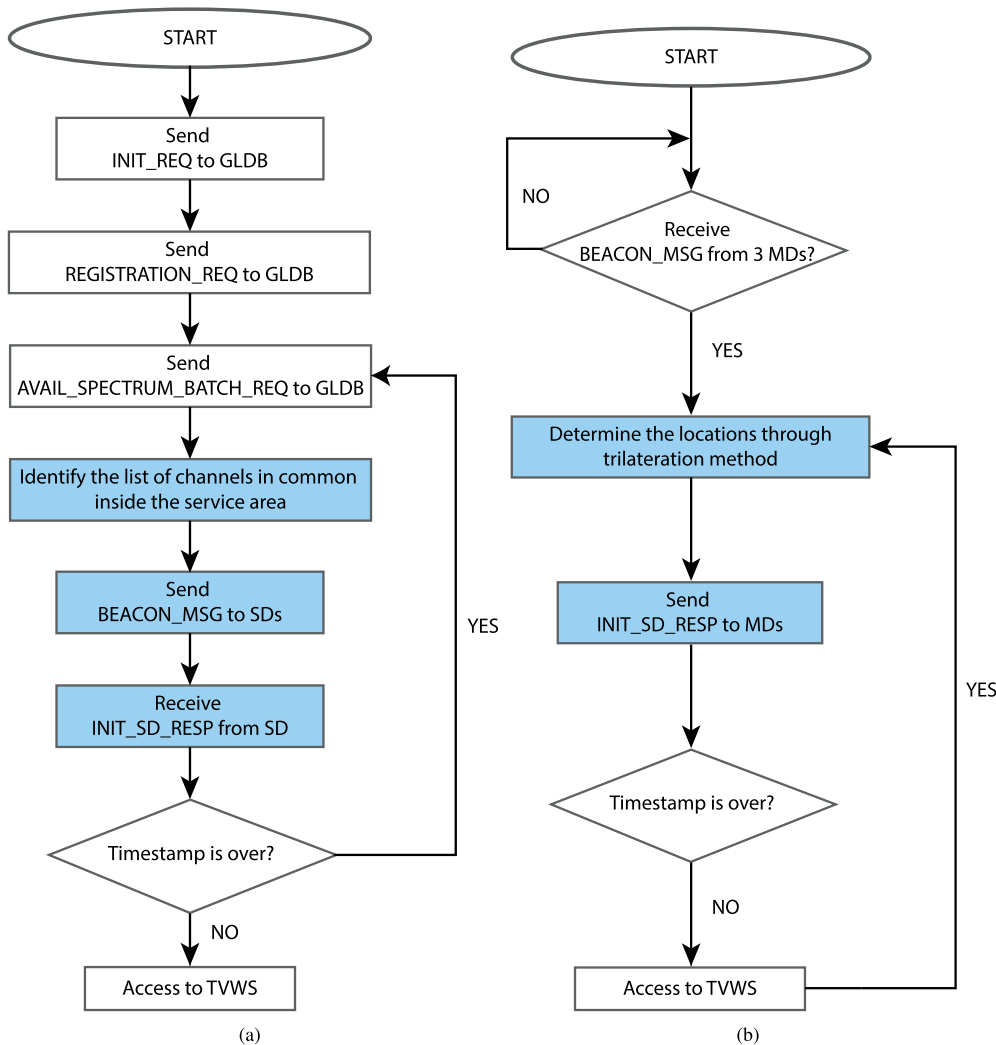


FIGURE 5. New steps proposal when the IoT device is inside to the deployment (a) master device (b) slave device.

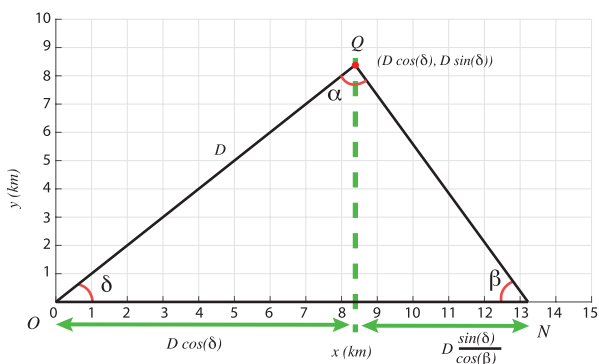


FIGURE 6. Area of the master device deployments.

above a given threshold θ_T . In this section, we consider only one receiver. Therefore, the packet loss probability $p_{L,i}$ between a slave device and master device i is given by:

$$p_{L,i} = \mathbb{P}(\theta_i < \theta_T). \tag{7}$$

where θ_i is the SNR on link i .

TABLE 3. Deployment cases.

| Triangle Index | α | β | δ |
|----------------|-----------|-----------|----------|
| 1 | $\pi/3$ | $\pi/3$ | $\pi/3$ |
| 2 | $5\pi/12$ | $\pi/3$ | $\pi/4$ |
| 3 | $\pi/2$ | $\pi/4$ | $\pi/4$ |
| 4 | $\pi/2$ | $\pi/3$ | $\pi/6$ |
| 5 | $\pi/2$ | $5\pi/12$ | $\pi/12$ |
| 6 | $7\pi/12$ | $\pi/4$ | $\pi/6$ |
| 7 | $7\pi/12$ | $\pi/3$ | $\pi/12$ |
| 8 | $2\pi/3$ | $\pi/6$ | $\pi/6$ |
| 9 | $2\pi/3$ | $\pi/4$ | $\pi/12$ |
| 10 | $3\pi/4$ | $\pi/6$ | $\pi/12$ |
| 11 | $5\pi/6$ | $\pi/12$ | $\pi/12$ |

Combining (4) and (6), we obtain

$$\theta_i = \frac{P_t}{N} \left(\frac{d_0}{r_i}\right)^\gamma 10^{\frac{\sigma_\xi}{10}} \chi \tag{8}$$

where r_i is the distance between the slave and master devices i .

Rewriting (8) into (7) for a given value of the fading, we have

$$\mathbb{P}(\theta_i < \theta_T | \chi = u) = \mathbb{P}\left(\xi \leq \frac{10}{\sigma} \log_{10} \left[\frac{\theta_T N}{P_T u} \left(\frac{r_i}{d_0}\right)^\gamma \right]\right), \quad (9)$$

thus,

$$\begin{aligned} \mathbb{P}(\theta_i < \theta_T | \chi = u) &= \frac{1}{2} \left(1 + \operatorname{erf} \left(\frac{10}{\sqrt{2}\sigma} \log_{10} \left[\frac{\theta_T N}{P_T u} \left(\frac{r_i}{d_0}\right)^\gamma \right] \right) \right) \end{aligned} \quad (10)$$

which can be re-written as

$$\begin{aligned} \mathbb{P}(\theta_i < \theta_T | \chi = u) &= \frac{1}{2} [1 + \operatorname{erf}(a_1 (b_2 - \ln(u)) + \gamma \ln r_i)]. \end{aligned} \quad (11)$$

with $a_1 = \frac{10}{\ln(10)\sigma\sqrt{2}}$ and $b_2 = \ln \frac{\theta_T N}{P_T d_0^\gamma}$.

The loss probability is the average for all fading values, then,

$$p_{L,i} = \int_0^{+\infty} \mathbb{P}(\theta_i < \theta_T | \chi = u) \exp(-u) du \quad (12)$$

When there is no fading, the loss probability is just given by (10) with $u = 1$.

D. SERVICE AREA

For each location, the loss probability can be computed either by (10) or (12). The outage probability p_o is defined as the packet loss probability over a given area. The service area S should fulfill the QoS objective, which is defined as the largest area for which the outage probability is smaller than a given threshold P_T .

The service area S is such that

$$p_o = \frac{\iint_S p_{L,i} ds}{S} \leq P_T. \quad (13)$$

E. REFERENCE SERVICE AREA

The reference case with which we compare our proposal is composed of one MD covering an area. As we assume omni-directional antennas, the service area is a disk and R represents the radius of this disk.

Equation (13) becomes

$$p_o = \frac{2}{R^2} \int_0^R p_L(r) r dr \quad (14)$$

where $p_{L,i}$ is rewritten as $p_L(r)$ to make the dependency with distance r clear and to avoid unnecessary indices.

By combining (11), (12) and (14), we obtain:

$$p_o = \frac{1}{R^2} \int_0^R \int_0^\infty [1 + \operatorname{erf}(a_1 (b_2 - \ln u) + \gamma \ln r)] \exp(-u) r du dr. \quad (15)$$

By switching the two integrals and using $x = r/R$, we have

$$p_o = \int_0^\infty \exp(-u) \int_0^1 [1 + \operatorname{erf}(A(u) + B \ln x)] x dx du. \quad (16)$$

with $A(u) = a_1 (b_2 + \gamma \ln R - \ln(u))$ and $B = a_1 \gamma$.

As shown in [28], the inside integral can be easily computed. We thus have:

$$p_o = \frac{1}{2} \int_0^\infty \exp(-u) \left[1 + \operatorname{erf}(A(u)) - \exp\left(\frac{1 - 2A(u)B}{B^2}\right) \times \left(1 + \operatorname{erf}\left(A(u) - \frac{1}{B}\right) \right) \right] du. \quad (17)$$

The closed formula for (18) is unknown, but the outage formula can be easily computed by any numerical method. When there is shadowing, but no fading, the outage probability is just given by:

$$p_o = \frac{1}{2} \left[1 + \operatorname{erf}(A(1)) - \exp\left(\frac{1 - 2A(1)B}{B^2}\right) \times \left(1 + \operatorname{erf}\left(A(1) - \frac{1}{B}\right) \right) \right]. \quad (18)$$

F. OUTAGE WITH THE PROPOSED ARCHITECTURE

When several MDs are used, the packet is received as soon as the SNR is above the threshold for at least one MD. Then,

$$P_L = P_{L,1} P_{L,2} P_{L,3} \quad (19)$$

As a result, the outage probability is given by

$$p_o = \frac{\iint_S P_{L,1} P_{L,2} P_{L,3} ds}{S}. \quad (20)$$

The outage formula depends on the deployment and on the considered service area. It is computed by a numerical method.

G. PERFORMANCE OF A LOADED NETWORK

The main performance indicator is the packet loss probability. As in the previous sections, we use a simple model to compute the transmission success probability p_s

$$p_s = \mathbb{P} \left\{ \text{SINR} = \frac{P_r}{I + N} \geq \theta_I \right\} \quad (21)$$

where I and N are the cumulative interference at the master device during packet transmission and the background noise power, respectively. The interference is due to all devices transmitting simultaneously and is computed with the propagation equation (4).

For our proposal with 3 MDs that can receive a packet, the success probability is given by

$$p_s = 1 - \prod_{i=1}^3 (1 - p_{s,i}) \quad (22)$$

where $p_{s,i}$ is computed with (21) by considering the power and the interference received at MD i .

Terminals are assumed to be located according to a Poisson Point Process (PPP) with spatial density λ_m in the service areas.

The radio interface is slotted and each device achieves synchronization by listening the beacon information. The slot duration is denoted by T .

TABLE 4. Model parameters.

| Parameter | Value | Comment |
|-----------------------|---------------|------------------------------|
| W | 125 kHz | Bandwidth |
| T | 10 ms | Slot duration |
| P_t | 20 dBm | Transmission power |
| f_{NF} | 3 dB | Noise factor |
| $\theta_T = \theta_I$ | 3 dB | SNR and SINR threshold |
| d_0 | 0.00057 km | Ref distance for propagation |
| γ | 3.377 | Propagation exponent |
| σ | 4 dB | St. dev. of shadowing |
| P_T | 1% | Outage objective |
| λ_u | 1 packet/hour | Traffic per device |

Our study is focused on massive IoT services with periodic reports. Each type of device has its own report period and, from an application point of view, devices are not synchronised. Thus, the global transmission process created by all devices can be approximated by a Poisson Process with parameter λ_s . Note that λ_s is the number of packets generated per second in the service area, which can either be a triangle as in section V-C or an hexagon as in section V-D.

Let λ_u be the average number of packets per time sent by a device, then, we have

$$\lambda_s = \lambda_m S \lambda_u \tag{23}$$

where S is the surface of the service area. The average load is thus

$$\rho = \lambda_s T = \lambda_m S \lambda_u T. \tag{24}$$

V. RESULTS AND ANALYSIS

In this section, we determine our reference parameters taking into account Section IV-E. Then, we analyze the basic configuration in which the service area is equal to the triangle deployment area, which allows identifying deployment rules. We then optimize our system by jointly determining the best deployment and service areas.

The analysis is made for the 500-MHz bandwidth, which is used for TV transmission. More precisely, the Okumura-Hata Model [29] is applied for a frequency equal to 584 MHz and the suburban area case. The transmission power of devices is 100 mW, which is equivalent to 20 dBm. Other parameters are shown in Table 4.

A. DETERMINATION OF THE REFERENCE CASE

The reference case consists of a single MD and a disk service area. By a simple iteration method, we determine the radius for which (18) gives a 1% outage. For shadowing only, the obtained values are $R = 4.2$ km and $S = 55.4$ km², while for shadowing effect with fast fading the values are $R = 1.98$ km and $S = 12.3$ km². According to Section IV-C, we show in Figure 7 the heat-maps of packet loss probability in one link in the reference areas.

B. SERVICE AREA RESTRICTED TO THE DEPLOYMENT TRIANGLE

We consider hereafter the simplest configuration: the service area is the triangle defined by the 3 MDs. The objective is

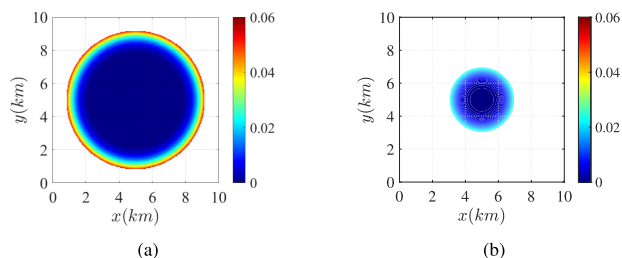


FIGURE 7. Packet loss probability in one link in the reference case with one MD: (a) shadowing and (b) shadowing with fast fading.

TABLE 5. Outage probability when the service area is restricted to the deployment triangle.

| Triangle Index | Outage with shadowing only | Outage with shadowing and fast fading |
|----------------|----------------------------|---------------------------------------|
| 1 | 0.0430 | 0.00089 |
| 2 | 0.0549 | 0.0011 |
| 3 | 0.0571 | 0.0013 |
| 4 | 0.1088 | 0.0025 |
| 5 | 0.3112 | 0.0187 |
| 6 | 0.0846 | 0.0024 |
| 7 | 0.2946 | 0.0181 |
| 8 | 0.0651 | 0.0027 |
| 9 | 0.2580 | 0.0167 |
| 10 | 0.1925 | 0.0136 |
| 11 | 0.1583 | 0.0117 |

to characterize the deployment that can provide an acceptable QoS. In order to make a fair comparison, we consider triangles that have the same area as our reference case (e.g. 55.4 km² with shadowing only, and 12.3 km² with shadowing with fast fading). We computed the outage probability according to (20) for each typical deployment with shadowing only and shadowing with fast fading. The results are shown in Table 5.

In the shadowing-only case, the outage with 3 MDs is larger than 1% in all cases. In the fast fading-case, the outage is reduced if compared with the reference case (i.e. it is lower than 1%) for triangle 1 – 4, 6 and 8. By analyzing Table 3, we deduce that such triangles are characterized by $\delta \geq \pi/6$. These configurations also give the lowest outage probability in the shadowing-only case. In the following, we will consider only deployments for which the smallest angle of the triangle is larger than $\pi/6$. In Figure 8, we show the packet loss probability in one link in the cases of $\delta \geq \pi/6$.

C. OPTIMIZATION OF THE TRIANGLE SERVICE AREA

In this section, our objective is to optimize the system. The transmission power and the noise level are kept constant. However, the size of the deployment triangle and of the service area is maximized while a maximum 1% outage probability is considered as a constraint.

In this part, the service area is still a triangle but larger than the deployment triangle. This new triangle can be defined by three points A , B and C as illustrated in Figure 9. Let R_D and R_S be the distances between the center of mass of the deployment triangle with the deployment top vertex (point Q) and the service-area top vertex (point C), respectively. D_A

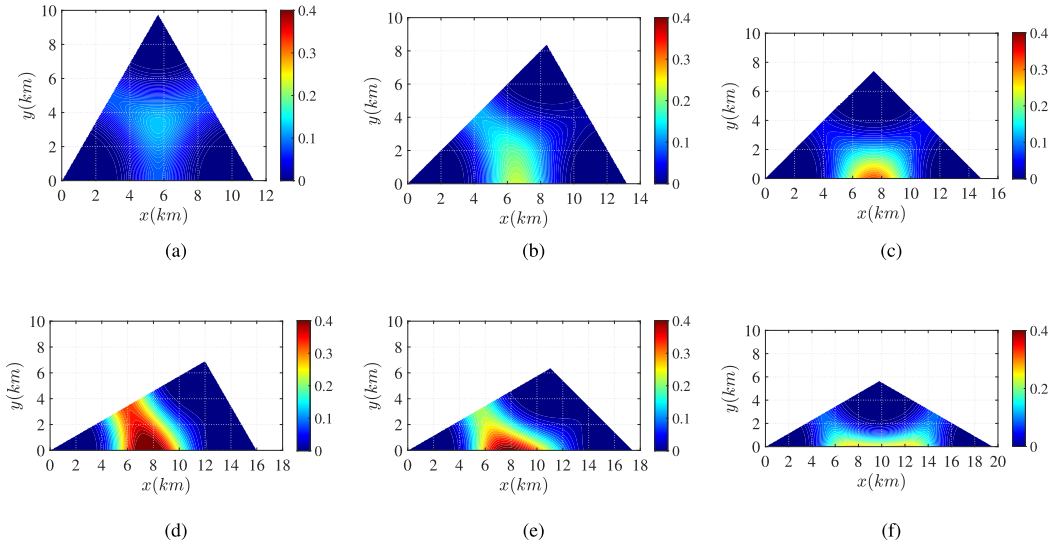


FIGURE 8. Packet loss probability in one link in deployment cases with 3 MDs characterized by $\delta \geq \pi/6$ with shadowing: (a) Deployment 1, (b) Deployment 2, (c) Deployment 3, (d) Deployment 4, (e) Deployment 6 and (f) Deployment 8.

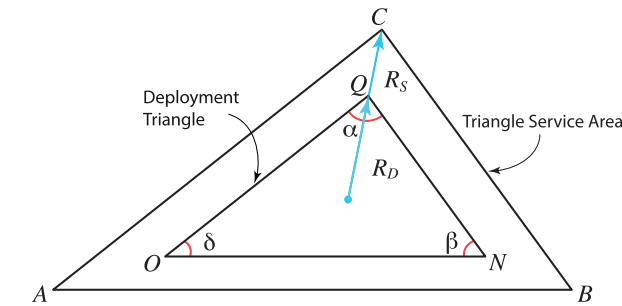


FIGURE 9. Deployment and service areas with R_D and R_S distance.

and S_A represent the deployment area and the triangle service area, respectively. In addition, we define p_o as the outage probability in the service area according to (20). In the case of the triangle service area S is equal to S_A .

The optimization can be written as

$$\max_{R_S, R_D} S_A \text{ s.t. } p_o \leq 10^{-2} \quad (25)$$

There are only 2 variables in the optimization process, then, an exhaustive research of the optimal solution is possible. Figures 10 and 11 show the variation of p_o for different values of R_S and R_D . The red points on Figures 10 and 11 represent the cases when p_o is equal to 0.01. The largest area is reached when $R_S = 11.22$ km and $R_D = 5.22$ km in triangle 1 with shadowing.

For the sake of brevity, not all the deployments are shown. We observed that for triangles 1 – 4, 6 and 8, there exist R_D and R_S values that reach the maximum outage constraint in (25).

In the proposed architecture, since there are 3 MDs instead of one in the reference case, the capital expenditure and the operational cost is higher. Covering the same area with a slightly lower outage probability is not enough to justify the additional investments required by the proposal. Consequently, we studied another shape of service area to improve the performance of our system.

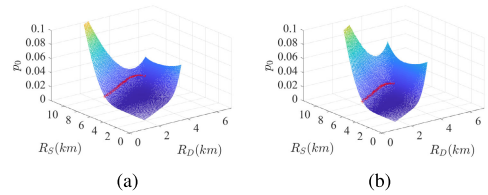


FIGURE 10. Outage packet loss probability considering shadowing with different R_S and R_D distances in examples of triangle service areas, red points show 1 % probability: (a) Triangle service Area 1, and (b) Triangle service Area 2.

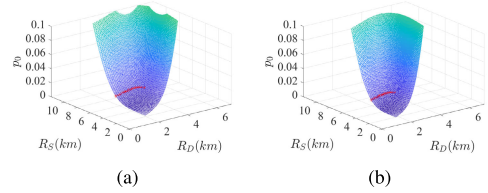


FIGURE 11. Outage packet loss probability considering shadowing and fast fading with different R_S and R_D distances in examples of triangle service areas. Red points show 1 % probability: (a) Triangle service Area 1 and (b) Triangle service Area 2.

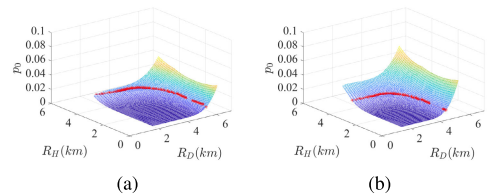


FIGURE 12. Outage packet loss probability considering shadowing with different R_H and R_D distances in examples of Hexagon service areas. Red points show 1 % probability: (a) Hexagon service Area 1 and (b) Hexagon service Area 2.

D. HEXAGON SERVICE AREA

We consider an hexagonal service area defined by points A to F . According to the deployment vertices (O, N, Q), we defined hexagon vertices. First, let L_0, L_1 and L_2 be the lines that join triangle vertices and R_H the distance between the triangle deployment and the hexagon service area (S_{Ah}) in Figure 14. In the case of the hexagon service area, S is equal to S_{Ah} .

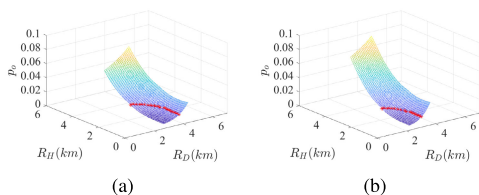


FIGURE 13. Outage packet loss probability considering shadowing with fast fading with different R_H and R_D distances in examples of Hexagon service areas. Red points show 1 % probability: (a) Hexagon service Area 1 and (b) Hexagon service Area 2.

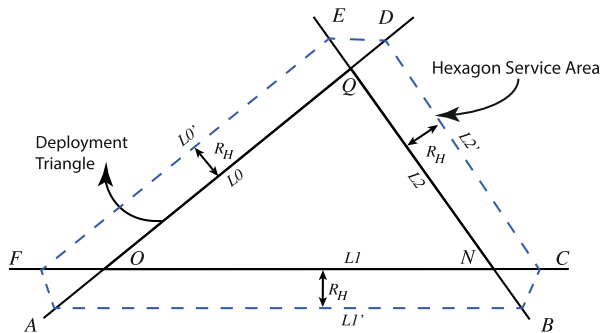


FIGURE 14. Hexagon service area.

The optimization goal can be written as

$$\max_{R_H, R_D} S_{Ah} \text{ s.t. } p_o \leq 10^{-2} \tag{26}$$

By following the same optimization process as in the triangle case, Figure 12 and 13 show the optimization results for the Hexagon service area considering R_H and R_D as the optimization variables. We obtained S_{Ah} values that satisfied the optimization goal described in (26).

E. SERVICE AREA RULES

The rules of the service area are defined considering the gain in the service area between the largest service area and the reference area (55.41 km² or 12.14 km², as mentioned in section V-A).

As shown in Figure 15, hexagons 1 – 3 in the shadowing case had a gain of more than 3 times. In the case of shadowing with fast fading case, the gain was larger than 3 in all hexagons and triangles evidenced in Figure 16. It is even larger than or equal to 6 for 3 deployment cases when the service area is an hexagon. Our objective is to provide the network access with our architecture to at least the same surface area per MD as an ideal system where each MD covers a disk area. To reach this objective, we can establish the following deployment rules. For a wide-band system (i.e. no fading), the service area should be a hexagon and the smallest angle of the deployment triangle should be larger than $\pi/4$. For a narrow-band system (i.e. with fast fading), the service area can be either a hexagon or a triangle and the smallest angle of the deployment triangle should be larger than $\pi/6$. In the latter case, if the angle is larger than $\pi/4$ and the service area is a hexagon, the surface area per MD can be doubled. In other words, with our proposal the same service area could be provided but with half of MDs.

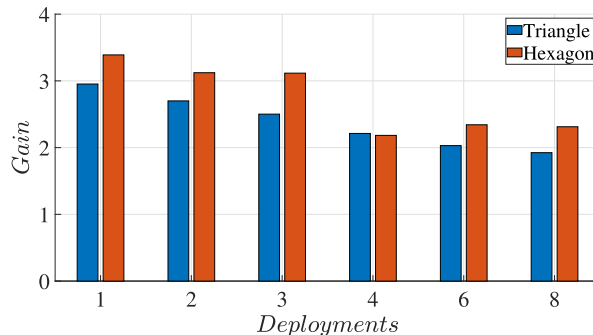


FIGURE 15. Gain of service areas considering shadowing.

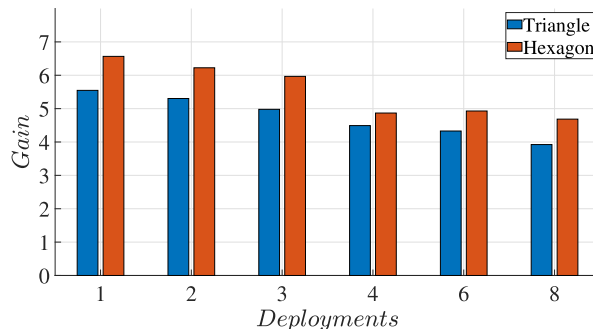


FIGURE 16. Gain of service areas considering shadowing with fast fading.

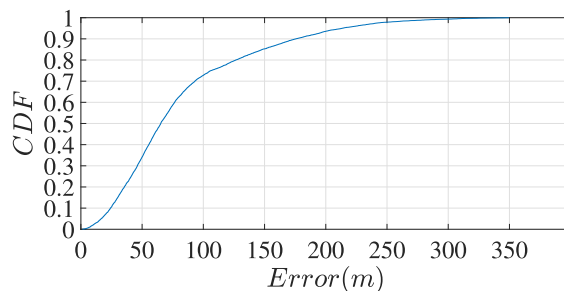


FIGURE 17. CDF error in IoT devices positioning.

F. IoT DEVICES POSITIONING

We simulate OTDOA considering the largest deployment and TOA correlation-based [27] with Zadoff-Chu sequences [30]. The location error was calculated considering the distance between the IoT location and hyperbolas intersection.

In Figure 17, the Cumulative Distribution Function (CDF) of location errors inside the deployment is presented. Results show that in 90% of the cases, the obtained OTDOA error is less than 200 meters and 70% of the cases reached less than 100 meters. Since in our access mechanism is particularly important to verify if the IoT end-device is inside the service area, by simulation results we verified that in 100% of the cases the end-devices were correctly located inside the service area.

G. PERFORMANCE ANALYSIS OF A LOADED SYSTEM

We analyzed the performance of the system for moderate to high load for the maximum hexagon service areas (Section V-E) and services with periodic reports [31]. The average packet loss probability is shown in Figure 18 considering our reference case with one MD and our proposal

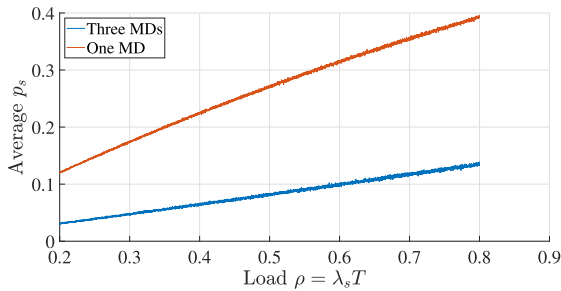


FIGURE 18. Average packet loss probability (for the whole service area).

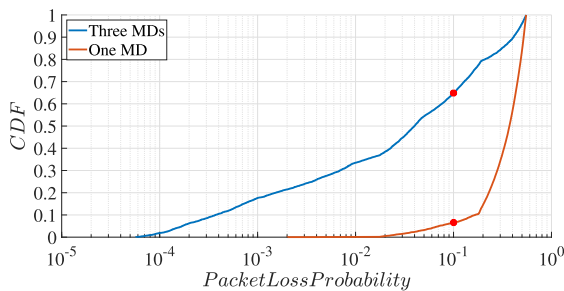


FIGURE 19. CDF p_s with load $\rho = 0.8$.

with three MDs. The load in this process is from 0.2 to 0.8. On the one hand, in the reference case the average packet loss probability is more than 10% in all load cases. In our proposal, with three MDs, average packet loss probability is equal to 10% when $\rho = 0.6$. On the other hand, when $\rho = 0.8$, in our reference case (i.e. one MD) the average packet loss is equal to 39.16% and in our proposal the average packet loss is equal to 13.57%.

The CDF of the packet loss probability is given in Figure 19 for our reference case (one MD) and our proposal (3 MDs) with the same load $\rho = 0.8$ in both cases. In the reference system, only 6% of the devices have a loss probability lower than or equal to 10%. In our system, this proportion is increased up to 65% and almost all devices have a loss probability of less than 10%. We evidenced that in our proposal we can guarantee some level of QoS considering packet loss probability for massive IoT services.

VI. CONCLUSION

We proposed a novel radio access mechanism that has the main features considering coexistence with TV primary user through GLDB and QoS constraints for defining *deployments* and *service areas*. Regarding *deployments* and *service areas*, first, we defined the reference case with respect to one MD topology. Then, we proposed service areas rules and a macro-diversity gain model.

The results were divided into four processes according to the outage probability of the following areas: triangle deployments, triangle service areas, triangle service areas improvement, and hexagon service areas. With respect to the triangle deployments and triangle service areas, we evidenced that in these processes the outage probability was not equal to 0.01 in their areas. However, we evidenced that after carrying out the optimization process of triangle service areas, it was

possible to find service areas with appropriate levels of outage probability in deployments with $\delta \geq \frac{\pi}{6}$. In terms of the hexagon service area, we implemented another optimization, it had optimal hexagons and improved the triangle service areas. Finally, we defined hexagon service area rules according to the deployment triangle angles. We concluded that with our proposal we could provide the same service area but with half of MDs, taking into account shadowing effect with fast fading and the reference case.

The performance of a loaded network in our proposal has the best values considering the average of packet loss probability and packet loss CDF with respect to the reference case with one MD. We can evidence that the average packet loss probability is reduced by 26% when the load is equal to 80% in our proposal. Therefore, we can guarantee some level of QoS for massive IoT services over TVWS.

About the future perspectives, there is a work in progress to develop a cognitive radio architecture based on this radio access mechanism for massive IoT over TVWS, which allows QoS constraints.

ACKNOWLEDGMENT

The authors would like to thank the cooperation of all partners within the Centro de Excelencia y Apropiación en Internet de las Cosas (CEA-IoT) Project.

REFERENCES

- [1] Ofcom. (May 2014). *M2M Application Characteristics and Their Implications for Spectrum Final Report*. [Online]. Available: http://stakeholders.ofcom.org.uk/binaries/research/technology-research/2014/M2M_FinalReportApril2014.pdf
- [2] J. Cabra, D. Castro, J. Colorado, D. Mendez, and L. Trujillo, "An IoT approach for wireless sensor networks applied to E-health environmental monitoring," in *Proc. 9th IEEE Int. Conf. Internet Things*, Jul. 2016, pp. 578–583.
- [3] D. Angulo-Esquerro, C. Villate-Barrera, W. Giral, H. C. Florez, A. T. Zona-Ortiz, and F. Diaz-Sanchez, "Parkurbike: An IoT-based system for bike parking occupation checking," in *Proc. IEEE Colombian Conf. Commun. Comput. (COLCOM)*, Aug. 2017, pp. 1–5.
- [4] M. A. Culman, J. A. Gomez, J. Talavera, L. A. Quiroz, L. E. Tobon, J. M. Aranda, L. E. Garreta, and C. J. Bayona, "A novel application for identification of nutrient deficiencies in oil palm using the Internet of Things," in *Proc. 5th IEEE Int. Conf. Mobile Cloud Comput., Services, Eng. (MobileCloud)*, Apr. 2017, pp. 169–172. [Online]. Available: <http://ieeexplore.ieee.org/document/7944891/>
- [5] C. A. Medina, M. R. Perez, and L. C. Trujillo, "IoT paradigm into the smart city vision: A survey," in *Proc. IEEE Int. Conf. Internet Things (iThings)*, Jun. 2017, pp. 695–704.
- [6] F. Montori, L. Bedogni, M. Di Felice, and L. Bononi, "Machine-to-machine wireless communication technologies for the Internet of Things: Taxonomy, comparison and open issues," *Pervasive Mobile Comput.*, vol. 50, pp. 56–81, Oct. 2018, doi: 10.1016/j.pmcj.2018.08.002.
- [7] *Internet Reports the Internet of Things*, ITU, Geneva, Switzerland, 2005.
- [8] *Overview of the Internet of Things*, ITU, Geneva, Switzerland, 2012.
- [9] *Deliverable D6.6 Final Report on the METIS 5G System Concept and Technology Roadmap*, Metis, Ontario, BC, USA, 2014.
- [10] P. Rawat, K. D. Singh, and J. M. Bonnin, "Cognitive radio for M2M and Internet of Things: A survey," *Comput. Commun.*, vol. 94, pp. 1–29, Nov. 2016.
- [11] D. Evans, "How the next evolution of the internet is changing everything," IoT, CISCO White Paper, Apr. 2011, pp. 1–78. [Online]. Available: https://www.cisco.com/c/dam/en_us/about/ac79/docs/innov/IoT_IBSG_0411FINAL.pdf
- [12] M. Perez, D. Jaramillo, D. Pinzon, and F. Herrera, "Spectrum forecasting model for IoT services," in *Proc. IEEE-APS Topical Conf. Antennas Propag. Wireless Commun. (APWC)*, Sep. 2018, pp. 877–881.

- [13] *A Spectrum Roadmap for IoT Opinion on the Spectrum Aspects of the Internet-of-Things (IoT) Including M2M*, European Commission, Brussels, Belgium, Nov. 2016.
- [14] A. Saifullah, M. Rahman, D. Ismail, C. Lu, J. Liu, and R. Chandra, "Low-power wide-area network over white spaces," *IEEE/ACM Trans. Netw.*, vol. 26, no. 4, pp. 1893–1906, Aug. 2018.
- [15] Y. Gao, Z. Qin, Z. Feng, Q. Zhang, O. Holland, and M. Dohler, "Scalable and reliable IoT enabled by dynamic spectrum management for M2M in LTE-A," *IEEE Internet Things J.*, vol. 3, no. 6, pp. 1135–1145, Dec. 2016.
- [16] W. Webb, *Understanding Weightless: Technology, Equipment, and Network Deployment for M2M Communications in White Space*. Cambridge, U.K.: Cambridge Univ. Press, 2012.
- [17] V. Chen, *Protocol to Access White-Space (PAWS) Databases*, document RFC 7545, 2015, pp. 1–90.
- [18] *FCC 10-174*, FCC, Washington, DC, USA, 2010.
- [19] R. Ramjee, S. Roy, and K. Chintalapudi, "A critique of FCC'S TV white space regulations," *GetMobile, Mobile Comput. Commun.*, vol. 20, no. 1, pp. 20–25, Jul. 2016.
- [20] Ofcom, "Licensing manually configurable white space devices statement," 2015, pp. 1–40. [Online]. Available: https://www.ofcom.org.uk/_data/assets/pdf_file/0023/84209/licensing_manually_configurable_white_space_devices.pdf
- [21] O. Holland, S. Ping, A. Aijaz, J. M. Chareau, P. Chawdhry, Y. Gao, Z. Qin, and H. Kokkinen, "To white space or not to white space: That is the trial within the Ofcom TV white spaces pilot," in *Proc. IEEE Int. Symp. Dyn. Spectr. Access Netw.*, Sep. 2015, pp. 11–22.
- [22] *ECC Report 159 Technical and Operational Requirements for the Possible Operation of Cognitive Radio Systems in the 'White Spaces' of the Frequency Band 470–790 MHz Cardiff, Wales, January 2011 'CEPT Has Subsequently Developed ECC Report 185 and 186 as Compe, TVWS*, Electron. Commun. Committee, Cardiff, U.K., Jan. 2011.
- [23] *ECC Report 236: Guidance for National Implementation of a Regulatory Framework for TV WSD Using Geo-Location Databases*, ECC, Erukkampattu, India, May 2015.
- [24] *Resolucion Nxtordmasculine 000105*, Agencia Nacional del Espectro, Bogotá, Colombia, 2020.
- [25] S. Fischer, "Observed time difference of arrival (OTDOA) positioning in 3GPP LTE," in *Proc. Qualcomm Technol.*, 2014, p. 62.
- [26] X. Lin, J. Bergman, F. Gunnarsson, O. Liberg, S. M. Razavi, H. S. Razaghi, H. Rydn, and Y. Sui, "Positioning for the Internet of Things: A 3GPP perspective," *IEEE Commun. Mag.*, vol. 55, no. 12, pp. 179–185, Dec. 2017.
- [27] M. Salomon, S. Lippuner, M. Korb, and Q. Huang, "Implementation and performance evaluation of cellular NB-IoT OTDOA positioning," in *Proc. IEEE/ION Position, Location Navigat. Symp. (PLANS)*, Apr. 2020, pp. 1365–1371.
- [28] C. Jakes, *Microwave Mobile*. New York, NY, USA: Wiley, 1974.
- [29] J. D. Parsons, "Fundamentals of VHF and UHF propagation," in *The Mobile Radio Propagation Channel*. Wiley, 2001, ch. 2, pp. 15–31. [Online]. Available: <https://onlinelibrary.wiley.com/doi/abs/10.1002/0470841524.ch2>, doi: 10.1002/0470841524.ch2.
- [30] R. Heimiller, "Phase shift pulse codes with good periodic correlation properties," *IRE Trans. Inf. Theory*, vol. 7, no. 4, pp. 254–257, Oct. 1961.
- [31] 3GPP, Valbone, France, Tech. Rep. Tr 45.820, 2015.



MANUEL PÉREZ (Member, IEEE) received the B.E. degree in electronics engineering from Pontificia Universidad Javeriana, Bogotá, Colombia, in 2009, as part of a double degree Program from the Politecnico di Torino, and the M.Sc. degree in wireless communications and the Ph.D. degree in electronics and communications engineering from the Politecnico di Torino, Italy, in 2010 and 2013, respectively. From 2009 to 2013, he was a Research Assistant with the iXem Labs (Politecnico di Torino) and the Laboratorio di Antenne e Compatibilità Elettromagnetica (LACE), Istituto Superiore Mario Boella (ISMB), Torino, Italy. He is currently an Associate Professor with the Electronics Department, Pontificia Universidad Javeriana. He has been also collaborated with the Centro de Excelencia y Apropiación en Internet de las Cosas (CEA-IoT) as a Team Director in the areas of wearables, smart cities, and safety, working in several I+D+i projects. His research interests include computational electromagnetics (CEM), antenna design, radar, the IoT, and electromagnetic compatibility (EMC).



TATIANA ZONA received the degree in telecommunication engineering from the Universidad Santo Tomás, Bogotá, Colombia, in 2002, and the M.Sc. degree in project management and the Ph.D. degree in telecommunications from the Universidad Politécnica de Valencia, Spain, in 2006 and 2008, respectively. She was a Researcher with the ITACA Institute, Universidad Politécnica de Valencia, Spain, from 2002 to 2007. Then, she was a Researcher and the Research and Development Manager at ITACA-CT with a TORRES QUEVEDO Grant, Valencia, Spain, until 2012. She is currently a Professor with the Telecommunication Engineering Faculty, Universidad Santo Tomás. She has been Santo Tomás Leader with the Centro de Excelencia y Apropiación en Internet de las Cosas (CEA-IoT), a Leader at the TVWS Database Project supported by ANE, and a researcher in several research and development projects in Spain and Colombia. Her research interests include research and development management, smart cities, the IoT, microwave heating, electromagnetic fields exposure, microwaves, and propagation.



MONICA ESPINOSA (Member, IEEE) received the B.E. degree in electronic engineering from Antonio Nariño University, in 2006, and the M.Sc. degree in magister in science in information and communications technology from Distrital University, Bogotá, Colombia, in 2013. She is currently pursuing the Ph.D. degree from the Centro de Excelencia y Apropiación en Internet de las Cosas (CEA-IoT), Javeriana University. She is currently a Professor in telecommunication engineering program with Santo Tomas University. Her research interests include television white spaces, the IoT, 4G, and 5G networks.



XAVIER LAGRANGE (Senior Member, IEEE) received the degree in engineering from the Ecole Centrale des Arts et Manufactures, Paris, France, in 1984, and the Ph.D. degree from TELECOM Paristech, in 1998. He is currently a Professor with IMT Atlantique (formerly known as Telecom Bretagne) and the Head of the ADOPNET Research Group, IRISA. He is a coauthor of several text books in French on wireless networks. His research interests include resource allocation, medium access control, and performance analysis for 4G and 5G cellular networks.

...